ARTICLE

OBC
www.rsc.org/obc

The stability of intramolecular DNA quadruplexes with extended loops forming inter- and intra-loop duplexes

Antonina Risitano and Keith R. Fox *

Division of Biochemistry & Molecular Biology, School of Biological Sciences, University of Southampton, Bassett Crescent East, Southampton, UK SO16 7PX. E-mail: K.R.Fox@soton.ac.uk; Fax: +44 23 8059 4459; Tel: +44 23 8059 4374

Received 28th February 2003, Accepted 22nd April 2003
First published as an Advance Article on the web 6th May 2003

We have examined the formation of intramolecular quadruplex DNA structures in which the loops have been extended so as to generate short DNA duplexes. Fluorescence melting and DNase I cleavage studies show that duplexes can be formed within each loop, but that duplexes between the loops are not stable.

Introduction

G-rich DNA sequences can fold to form four-stranded DNA structures, known as quadruplexes (tetraplexes), which contain stacks of G-quartets.[1–3] These structures may be adopted by telomeric DNA repeats[4,5] as well as other genetic control regions[6–10] and form the platform for folding of several aptamer molecules.[11–14] Some of these folded structures contain interactions between bases within the loops that connect the different strands.[6,10] We have examined whether these loops can be extended to form DNA duplexes and have prepared oligonucleotides which have the potential for forming duplexes between the two arms of each loop (intra-loop) or between adjacent loops (inter-loop). Models for how these oligonucleotides might fold are shown in Fig. 1. The stability of these structures was examined by determining their thermal melting profiles under different ionic conditions while the location of duplex regions was assessed by cleavage with DNase I.

Results

Fluorescence melting studies

We have previously shown that quadruplex DNA melting profiles can be measured using oligonucleotides containing appropriately placed fluorophores and quenchers using a LightCycler.[15] When the oligonucleotide is folded the fluorophore and quencher are in close proximity and the fluorescence is quenched. When the strands separate the fluorophore and quencher are a large distance apart and there is a large increase in fluorescence signal. Melting profiles for the inter- and intra-loop oligonucleotides, together with the human telomeric repeat sequence are shown in Fig. 2 in sodium- and potassium-containing buffers, and the T_m values are summarised in Table 1. Both oligonucleotides produce clear fluorescence melting transitions under all the conditions employed, confirming that the oligonucleotides have folded into a configuration in which the fluorophore and quencher are in close proximity. It can be seen that the intra- and inter-loop oligonucleotides melt at lower temperatures than the human telomeric repeat sequence under all conditions tested. The T_m values for the intra-loop and human telomere sequences are higher in the presence of potassium than sodium, as expected for structures that contain G-quartets. In contrast the inter-loop has the same T_m in both potassium- and sodium-containing buffers.

We have previously shown that the human telomeric sequence shows hysteresis between the heating and melting profiles,[15] and that the T_m values estimated from annealing are lower than those determined from the melting curves. This is caused by the slow rate of folding and unfolding of these complexes, so that the reaction is not at thermodynamic equilibrium during the heating and cooling cycles (in which the temperature is changed at 0.1 °C s^{-1}). This hysteresis is most apparent at low potassium concentrations and is not observed in the presence of sodium. It can be seen (Fig. 2) that the intra-loop oligonucleotide displays a similar pattern of hysteresis, while there

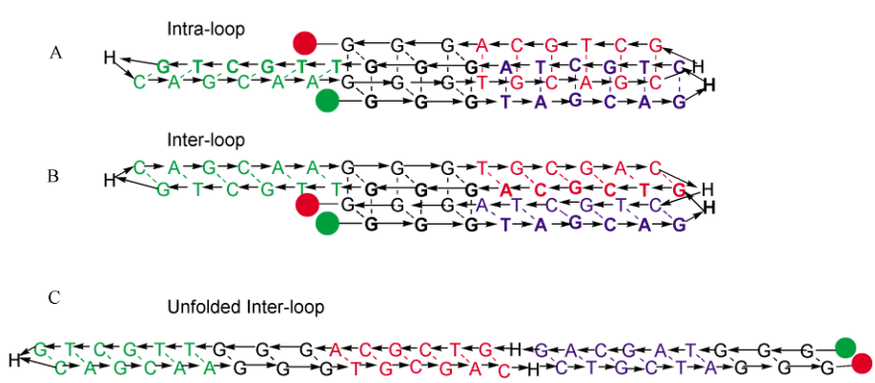

Fig. 1 Possible folding patterns of the oligonucleotides designed to form inter- and intra-loop structures. The arrows indicate the polarity of the DNA strands, running from 5′ to 3′. The sequences are labeled at the 3′-end with dR-MeRed (red circle) and with dR-FAM (green circle) at the 5′-end. H = hexaethylene glycol linker. The various mini-duplexes are shown in different colors. The arrows show the oligonucleotide backbone in the direction 5′–3′. For the intra-loop this can be traced as 5′-FAM-GGGTAGCAG-H-CTGCTAGGGTTGCTG-H-CAGCAAGGGTGCAGC-H-GCTGCAGGG-MeRed, while for the inter-loop this is 5′-FAM-GGGTAGCAG-H-GTCGCAGGGTTGCTG-H-CAGCAAGGGTGCGAC-H-CTGCTAGGG-MeRed. A) Folded structure for the intra-loop oligonucleotide, generating an intramolecular quadruplex with mini-duplexes formed within each extended loop. B) Folded structure for the inter-loop quadruplex, generating an intramolecular quadruplex with mini-duplexes formed between the extended loops. C) Unfolded structure of the inter-loop oligonucleotide forming an intramolecular duplex.

DOI: 10.1039/b302251j

Table 1 T_m values (K) for melting and annealing of the various intramolecular quadruplexes. All experiments were buffered at pH 7.4

	Intra-loop		Inter-loop		$(GGGTTA)_3GGG$	
	Melt	Anneal	Melt	Anneal	Melt	Anneal
50 mM Potassium phosphate	328	325	325	326	346	345
50 mM Sodium phosphate	319	318	327	327	329	328
50 mM Potassium phosphate + 1 mM $MgCl_2$	330	327	327	327	346	345
10 mM Lithium phosphate	Too low to measure	Too low to measure	316	315	Too low to measure	Too low to measure
10 mM Lithium phosphate + 10 mM LiCl	314	311	320	319	Too low to measure	Too low to measure
10 mM Lithium phosphate + 40 mM LiCl	320	318	327	327	310	310
10 mM Lithium phosphate + 10 mM KCl	319	311	318	318	330	325
10 mM Lithium phosphate + 40 mM KCl	319	321	324	324	340	336

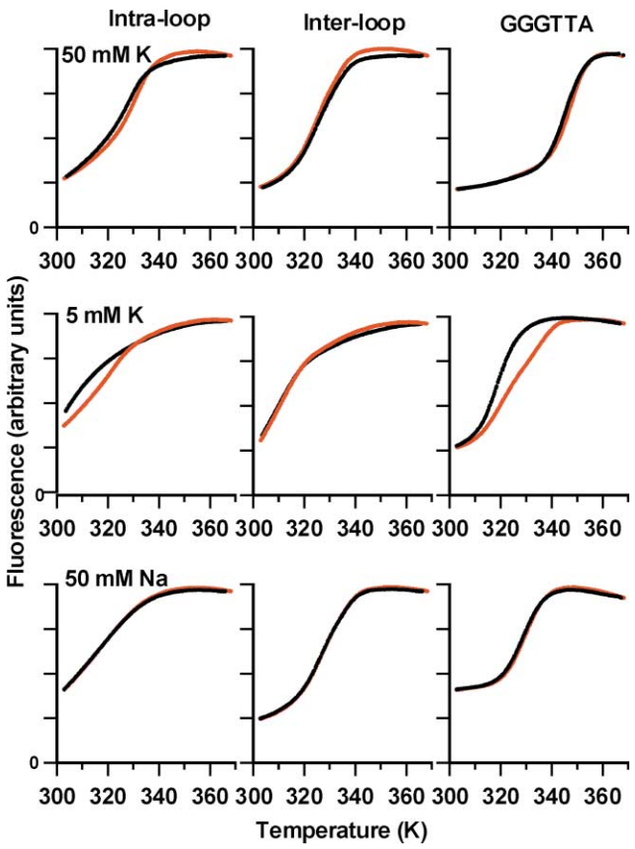

Fig. 2 Fluorescence melting and annealing profiles for the intra-loop (first column) and inter-loop (middle column) oligonucleotides, together with data for the human telomeric repeat sequence (GGGTTA) with TTA in the loops (right hand column). The red curves are melting profiles while the black are annealing profiles. The *y*-axis shows the normalized relative fluorescence. The experiments were performed in 50 mM potassium phosphate pH 7.4 (first row), 5 mM potassium phosphate pH 7.4 (middle row) or 50 mM sodium phosphate pH 7.4 (bottom row).

are no differences in the heating and annealing profiles for the inter-loop. These results again suggest that the intra-loop oligonucleotide contains a typical G-quadruplex, while the inter-loop does not. The presence of duplex regions in the folded structures of the inter- and intra-loop oligonucleotides is also suggested by the observation that addition of 1 mM $MgCl_2$ increases their T_m values by about 2 K. In contrast this concentration of magnesium has no effect on the human telomeric repeat sequence. Higher concentrations of $MgCl_2$ (10 mM) stabilize all three oligonucleotides, though the intra- and inter-loop are stabilized more than the human telomeric sequence. Similarly we find that the intra- and inter-loop structures are both stabilized by ethidium bromide and actinomycin D, while these ligands have no effect on the human quadruplex sequence (not shown).

It is well known that quadruplexes are much less stable in the presence of lithium ions and the order of stabilization is $K^+ > Na^+ >> Li^+$.[16] We therefore performed similar experiments in lithium-containing buffers and the results are shown in Fig. 3 and Table 1. It can be seen that both the human telomeric and the intra-loop sequences are destabilized by the presence of lithium and a large part of the melting transition occurs below 300 K. Addition of potassium restores the melting transitions in a concentration dependent fashion. This cannot be simply due to increased ionic strength as the addition of equivalent amounts of lithium has only a small effect on T_m. Again these melting curves show hysteresis between the melting and annealing. In contrast lithium has little or no effect on the melting of the inter-loop sequence and the T_m is increased by a similar amount on adding potassium or lithium. These results again suggest that the human telomeric and intra-loop sequences contain quadruplex structures, while the inter-loop does not.

Gel mobility

We confirmed that the inter- and intra-loop oligonucleotides adopt different structures by comparing their mobilities on non-denaturing polyacrylamide gels (Fig. 4A). Since these two oligonucleotides are the same length, any differences in mobility must reflect their different folding patterns. It can be seen that, in the presence of 50 mM KCl, the inter-loop has about 20% faster mobility.

DNase I cleavage

The structure of these folded oligonucleotides was also studied by examining their cleavage by DNase I. This enzyme should cut in the duplex portions, while the stacked G-quartets should be refractory to cleavage. The cleavage patterns with DNase I are shown in Fig. 4. It can be seen that the intra-loop produces the expected cleavage pattern with no cutting in the G-tracts. In contrast there is significant cleavage within the G-tracts of the inter-loop, suggesting that these are not involved in G-quadruplexes.

Discussion

The melting profiles for the intra-loop oligonucleotide suggest that this does indeed fold into a quadruplex structure, containing duplexes in the extended loop. Its T_m values are higher in potassium than sodium and it is destabilized by addition of lithium; the observed hysteresis suggests that it contains a complex structure which is slow to form and there is no DNase I cleavage within the G-tracts. These properties are similar to those of the human telomeric sequence. In contrast the data for the inter-loop sequence are not consistent with quadruplex formation; the melting curves are similar in sodium-, potassium- and lithium-containing buffers and there is DNase I cleavage within the G-tracts. We suggest that this forms an

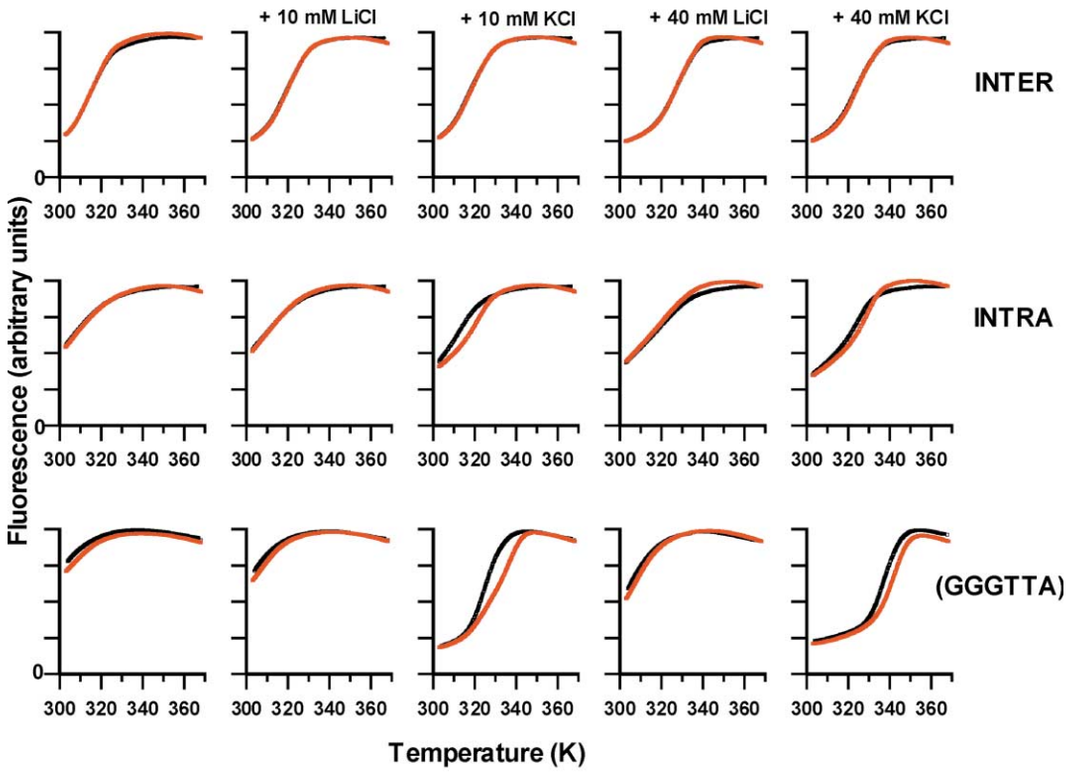

Fig. 3 Fluorescence melting and annealing profiles for the intra- and inter-loop oligonucleotides, together with data for the human telomeric repeat sequence (GGGTTA) measured in lithium-containing buffers. The red curves are melting profiles while the black are annealing profiles. The *y*-axis shows the normalized relative fluorescence. All reactions were performed in 10 mM lithium phosphate pH 7.4, containing 0, 10 or 40 mM LiCl or KCl.

extended hairpin duplex by unpairing through the center of the folded structure generating the unfolded hairpin duplex shown in Fig. 1C. This hairpin duplex contains several G.G mismatches. In the usual quadruplex representation the central loop (the left hand loop in Fig. 1A) crosses the stacked quartets. This crossed arrangement is not accessible for the inter-loop as the duplexes between adjacent loops would have a parallel rather than an antiparallel arrangement. In contrast the intra-loop sequence could form either crossed or uncrossed structures. It is possible that crossing the strands at the central loop provides added stability to the structure. It should be noted that a recent crystal structure of the human telomere sequence suggests that all four strands are parallel.[5] This arrangement would also permit the formation of the intra- but not the inter-loop structure.

Experimental

Oligonucleotides

Oligonucleotides were purchased from Oswel DNA service, Southampton, UK and were purified by gel electrophoresis. Oligonucleotides for the fluorescence melting experiments contained a fluorophore (fluorescein, dR-FAM) at the 5′-end and a quencher (Methyl Red, dR-MeRed) at the 3′-end. These fluorophores are positioned so that, when the oligonucleotide folds into the structures shown in Fig. 1, they are in close proximity and the fluorescence is quenched. When these structures unfold the fluorophore and quencher are separated by a large distance and there is a large increase in fluorescence. The sequences of the oligonucleotides were: intra-loop, 5′-dRFam-GGGTAG-CAG-H-CTGCTAGGGTTGCTG-H-CAGCAAGGGTGCA-GC-H-GCTGCAGGG-dRMeRed, while for the inter-loop this is 5′-dRFam-GGGTAGCAG-H-GTCGCAGGGTTGCTG-H-CAGCAAGGGTGCGAC-H-CTGCTAGGG-dRMeRed, (H = hexaethylene glycol). The intended folded conformations of these oligonucleotides are shown in Fig. 1. The human telomeric DNA sequence, which was used in our previous studies,[15] has the sequence dRMeRed-GGGTTAGGGTTAGGGT-TAGGG-dRFam.

The oligonucleotides used for the DNase I cleavage experiments contained the same DNA sequences, without the fluorophore and quencher, but with an additional T_{10} attached to the 5′-end to enable resolution of all the bands in the quadruplex region on a polyacrylamide gel. These oligonucleotides were labeled at the 5′-end using γ-^{32}P-ATP and polynucleotide kinase. The radiolabelled species were purified on denaturing polyacrylamide gels.

Fluorescence melting studies

Fluorescence melting curves were determined in a Roche LightCycler as previously described,[15] using a total reaction volume of 20 μL. For each reaction the final oligonucleotide concentration was 0.25 μM, diluted in an appropriate buffer. In a typical experiment the samples were first denatured by heating to 95 °C at a rate of 0.1 °C per second. The samples were then maintained at 95 °C for 5 minutes before annealing by cooling to 25 °C at 0.1 °C per second (this is the slowest heating and cooling rate for the LightCycler). They were held at 25 °C for a further 5 minutes and then melted by heating to 95 °C at 0.1 °C per second. Recordings were taken during both the melting steps as well as during the annealing. The LightCycler has one excitation source (488 nm) and three channels for recording fluorescence emission at 520, 640 and 705 nm. For the studies in this work we measured the changes in fluorescence at 520 nm. T_m values were determined from the first derivatives of the melting profiles using the Roche LightCycler software. Each reaction was performed in triplicate and the T_m values usually differed by less than 0.5 °C.

DNase I cleavage

Radiolabelled oligonucleotides (3 μL) were diluted in 50 mM sodium (or potassium) phosphate buffer pH 7.4. These were

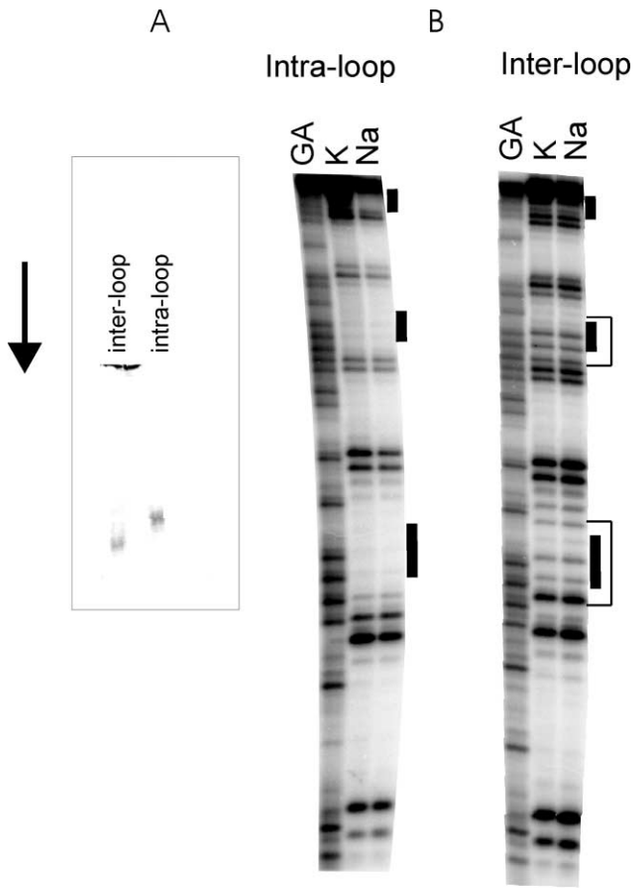

Fig. 4 A) Mobility of the intra- and inter-loop oligonucleotides in non-denaturing polyacrylamide gel electrophoresis. 3 μl of each oligonucleotide (10 μM) dissolved in 50 mM potassium phosphate pH 7.4 were loaded into each lane of a 10% polyacrylamide. The gel and running buffer were made with TBE buffer which had been supplemented with 50 mM KCl. The arrow shows the direction of electrophoresis. B) DNase I digestion patterns for the inter- and intra-loop complexes. Tracks labeled K and Na correspond to 50 mM potassium phosphate or 50 mM sodium phosphate respectively. The DNA was labeled at the 5′-end with ^{32}P. The 5′-end of these oligonucleotides contained an additional ten T residues to enable resolution of the bands on the gel. Tracks labeled GA are markers specific for G and A. The bars indicate the location of the blocks of G-residues in the DNase I cleavage patterns. Note that the products of DNase I digestion run slower than the marker lanes as DNase I generates labelled fragments with a hydroxyl group at the 3′-end while the products of Maxam–Gilbert sequencing reactions have a 3′-phosphate. This difference is greatest for shorter fragments. The brackets indicate the regions where DNase I products are found in the inter-loop, but not the intra-loop.

digested by adding 2 μL DNase I, which had been diluted in 20 mM NaCl, 2 mM $MgCl_2$, 2 mM $MnCl_2$ at a concentration of about 0.01 units ml^{-1}. The reaction was stopped after 1 minute by adding 4 μL of a formamide solution containing 10 mM EDTA and 0.1% (w/v) bromphenol blue. The samples were heated at 100 °C for 3 minutes and resolved on a 16% polyacrylamide gel containing 8 M urea. After electrophoresis the gels were fixed in 10% (v/v) acetic acid, transferred to Whatmann 3MM paper and dried under vacuum at 80 °C. The dried gels were exposed to a Kodak storage phosphor screen, which was scanned using a Molecular Dynamics Storm 860 phosphorimager. Bands in the digest were assigned by comparison with Maxam–Gilbert marker lanes specific for purines. It should be noted that DNase I generates labelled fragments with a hydroxyl group at the 3′-end while the products of Maxam–Gilbert sequencing reactions have a 3′-phosphate. As a result the products of DNase I digestion run slower than the marker lanes; this difference is greatest for shorter fragments.

Acknowledgements

This work was supported by a grant from the European Union. The LightCycler was partly funded by the BBSRC (JREI).

References

1 J. R. Williamson, *Curr. Opin. Struct. Biol.*, 1993, **3**, 357–362.
2 M. A. Keniry, *Biopolymers*, 2000, **56**, 123–146.
3 T. Simonsson, *Biol. Chem.*, 2001, **382**, 621–628.
4 Y. Wang and D. J. Patel, *Structure*, 1993, **1**, 263–282.
5 G. N. Parkinson, M. P. H. Lee and S. Neidle, *Nature*, 2002, **417**, 876–880.
6 T. Simonsson, P. Pecinka and M. Kubista, *Nucleic Acids Res.*, 1998, **26**, 1167–1172.
7 A. Rangan, O. Y. Fedoroff and L. H. Hurley, *J. Biol. Chem.*, 2001, **276**, 4640–4646.
8 D. Sen and W. Gilbert, *Nature*, 1988, **334**, 364–366.
9 P. Catasti, X. Chen, R. K. Moyzis, E. M. Bradbury and G. Gupta, *J. Mol. Biol.*, 1996, **264**, 534–545.
10 A. Rangan, O. Fedoroff and L. H. Hurley, *J. Biol. Chem.*, 2001, **276**, 4640–4646.
11 I. Smirnov and R. H. Shafer, *Biochemistry*, 2000, **39**, 1462–1468.
12 P. Schultze, R. F. Macaya and J. Feigon, *J. Mol. Biol.*, 1993, **235**, 1532–1547.
13 N. Jing and M. E. Hogan, *J. Biol. Chem.*, 1998, **273**, 34992–34999.
14 N. Jing, R. F. Rando, Y. Pommier and M. E. Hogan, *Biochemistry*, 1997, **36**, 12498–12505.
15 R. A. J. Darby, M. Sollogoub, C. McKeen, L. Brown, A. Risitano, N. Brown, C. Barton, T. Brown and K. R. Fox, *Nucleic Acids Res.*, 2002, **30**, e39.
16 W. S. Ross and C. C. Hardin, *J. Am. Chem. Soc.*, 1994, **116**, 6070–6080.